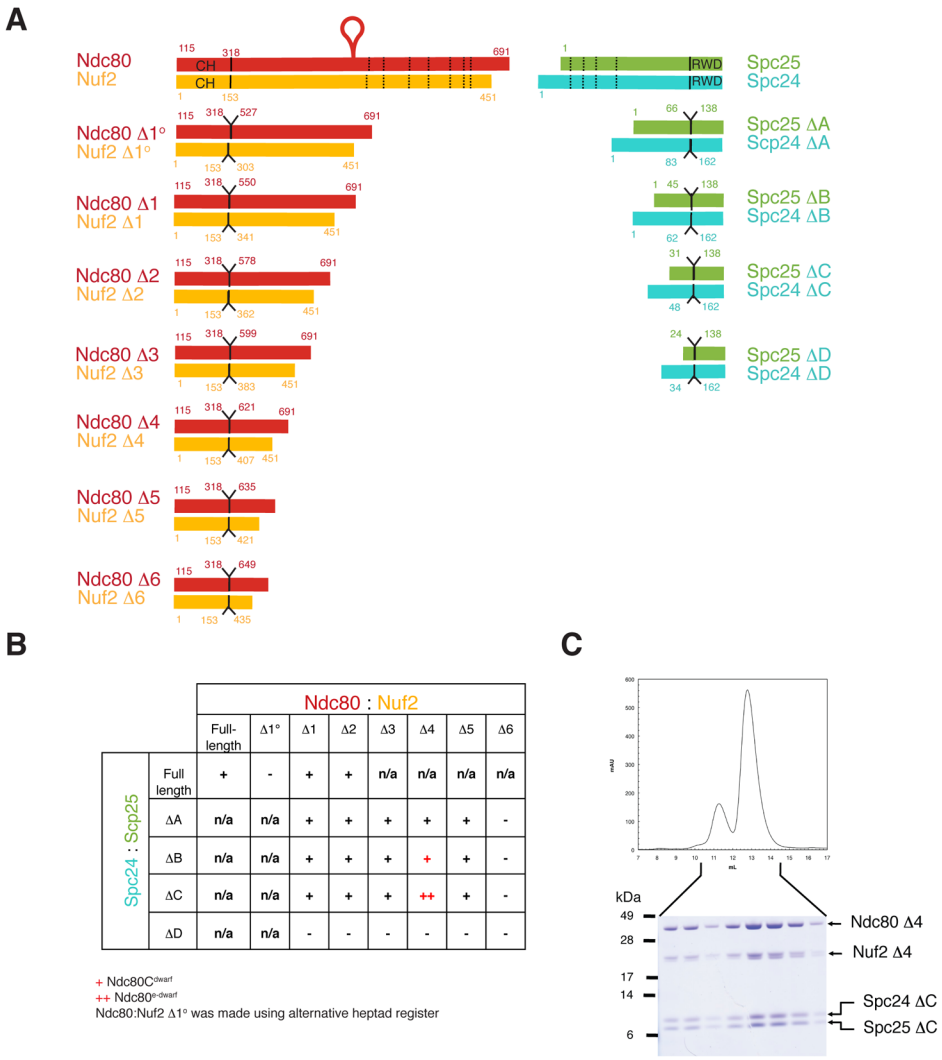

Spc24 : Spc25 \ Ndc80 : Nuf2	Full-length	Δ1°	Δ1	Δ2	Δ3	Δ4	Δ5	Δ6
Full length	+	-	+	+	n/a	n/a	n/a	n/a
ΔA	n/a	n/a	+	+	+	+	+	-
ΔB	n/a	n/a	+	+	+	+	+	-
ΔC	n/a	n/a	+	+	+	++	+	-
ΔD	n/a	n/a	-	-	-	-	-	-

+ Ndc80C^{dwarf}
++ Ndc80$^{e\text{-}dwarf}$
Ndc80:Nuf2 Δ1° was made using alternative heptad register

Figure S1, related to Experimental Procedures. Ndc80c constructs.

(A) Diagram of deletions. Numbers indicate points of fusion in shortened versions of each heterodimer. For example, residues 115-318 of Ndc80 were fused to residue 621, and residues 1 – 153 of Nuf2 were fused to 407 to make the Ndc80D4:Nuf2D4 heterodimer. (B) Combination of shortened Ndc80:Nuf2 and Spc24:Spc25. Pairs were co-expressed with a N-terminal His-tag on the Ndc80 and Nuf2 polypeptides. Plus sign: tetramer formation; minus sign: no tetramer detected. Ndc80D4:Nuf2D4 and Spc24DB:Spc25DB form a stable tetramer referred to as Ndc80c^{dwarf} in the main text. Ndc80D4:Nuf2D4 and Spc24DC:Spc25DC form Ndc80c$^{e\text{-}dwarf}$. (C) Size exclusion chromatography elution profile of Ndc80c$^{e\text{-}dwarf}$. Peaks resolved on SDS-PAGE. Fractions constituting the second peak (12 – 14 mL) were pooled and concentrated for crystallization and binding studies.

A

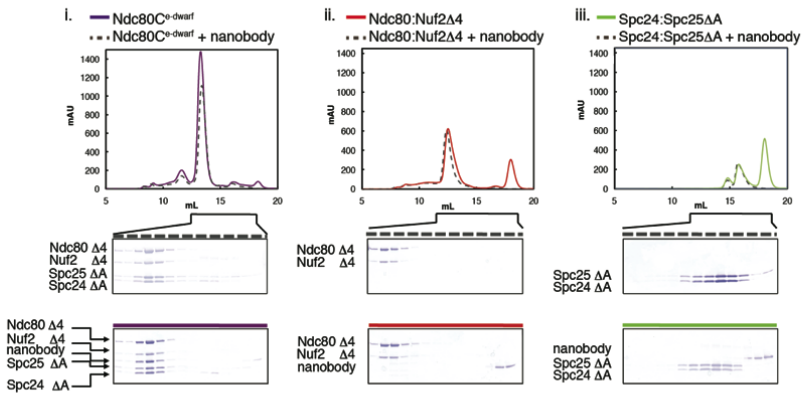

B

	Ndc80 (115-318) Nuf2 (1-152)	Spc24 (162 -213) Spc25 (138 - 221)
Ndc80 (115-318) Nuf2 (1-152)	-	-
Spc24 (162 -213) Spc25 (138 - 221)	-	-
Nanobody	-	-

C

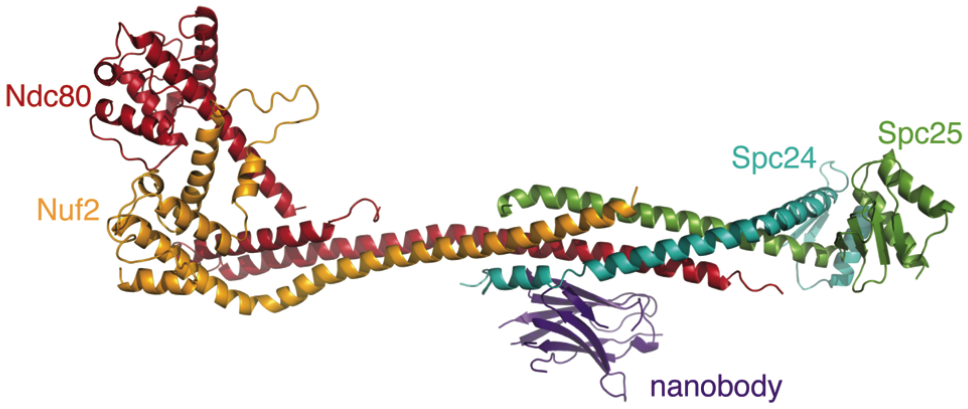

Figure S2, related to Figure 2 and Experimental Procedures. Nanobody binds Ndc80c tetramer junction.
(A) Size exclusion chromatography elution profiles and SDS-PAGE analyses: (i) Ndc80c$^{e\text{-}dwarf}$ components (gray line); 1:1 stoichiometric mixture with nanobody (purple solid line); ii: Ndc80D4:Nuf2D4 (gray line); 1:1 stoichiometric mixture with nanobody (red line); iii: SpcDA24:Spc25DA (gray line) and 1:1 stoichiometric mixture with nanobody. (B) Summary of mixtures assayed for complex formation by gel filtration (data not shown). Nanobody does not bind either globular end of Ndc80c$^{e\text{-}dwarf}$. The globular ends of Ndc80c$^{e\text{-}dwarf}$ do not dimerize or interact with each other. (C) Structure of Ndc80c$^{e\text{-}dwarf}$ with bound nanobody.

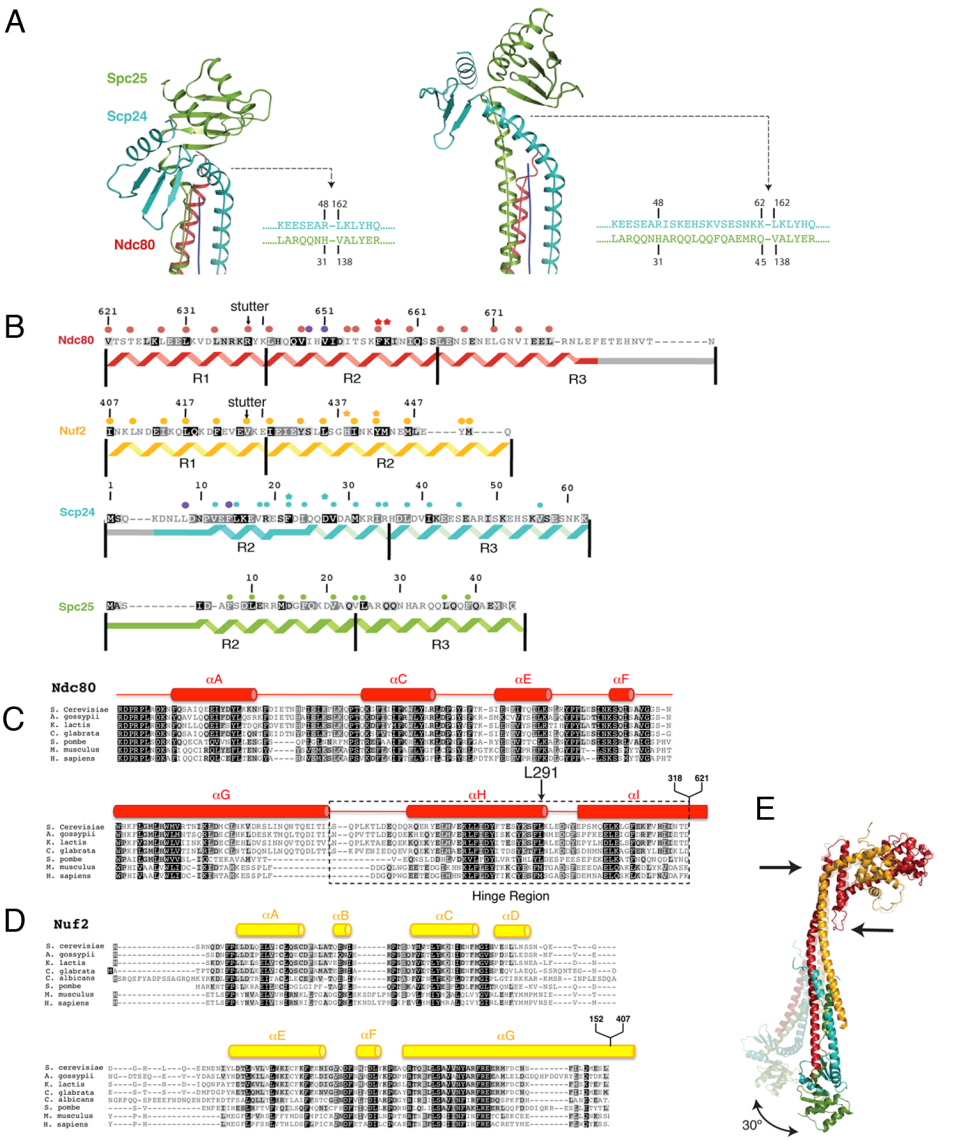

Figure S3, related to Figures 3 and 4. Various features of the Ndc80c$^{dwarf/e\text{-}dwarf}$ structures.
(A) Paired RWD heterodimer of Spc24-Spc25; the angle with respect to central axis is due to a 6-residue longer coiled-coil in the Spc24 constructs we used. Left: Ndc80c^{dwarf}; right: Ndc80c$^{e\text{-}dwarf}$. (B)-(D). Alignment of Ndc80 and Nuf2 sequences, annotated with secondary structural elements from the Ndc80c$^{dwarf/e\text{-}dwarf}$ structures. (B) Sequence of *S. cerevisiae* Ndc80c components, with boundaries as in **Figure 3A**. Black and gray boxes show conservation among all fungal species for which sequences are known (with gradation from black to white corresponding to decreasing extent of conservation). Solid colored circles above residues: buried amino acids. Asterisks: interacting residues shown in **Figure 3B**. Solid gray circles: residues in the hydrophobic surface contacted by the nanobody. (C) Alignment of Ndc80 sequences, spanning residues 115 – 318 of *S. cerevisiae* Ndc80. (D) Alignment of Nuf2 sequences, spanning residues 1 – 33 of *S. cerevisiae* Nuf2. (E) Ndc80c^{dwarf} aligned with Ndc80c$^{e\text{-}dwarf}$ on residues spanning the hinge region (marked by black arrows).

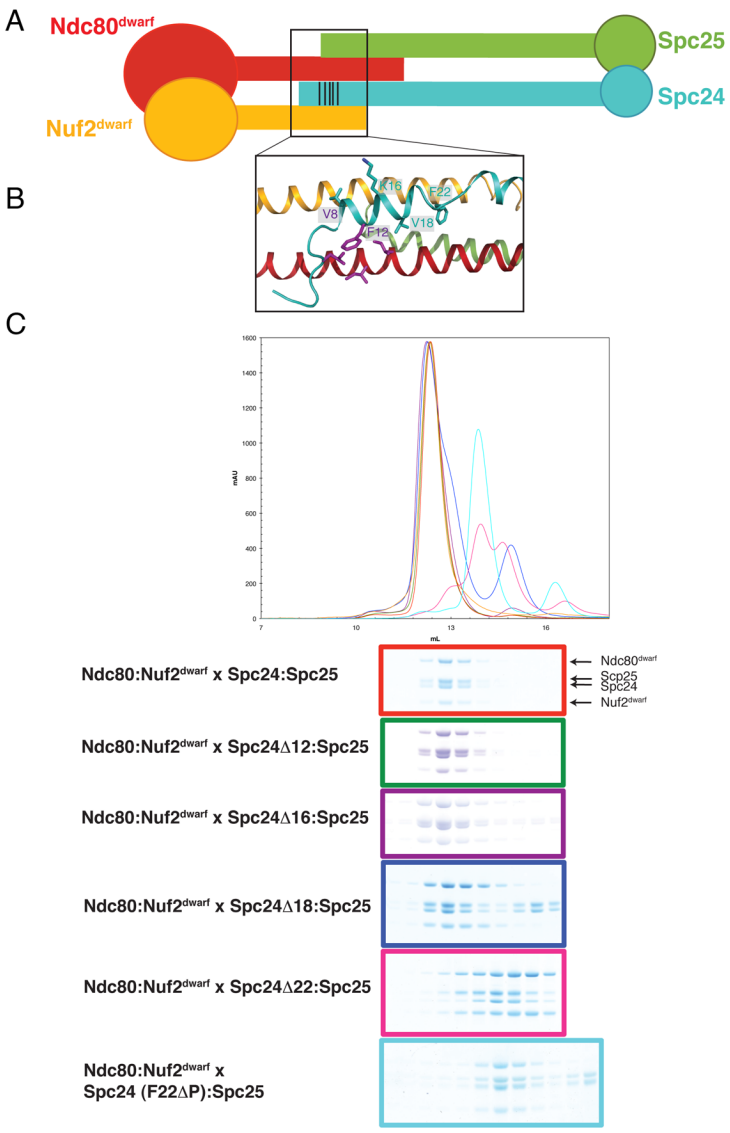

Figure S4, related to Figure 3. Mutational analysis of the Ndc80c junction. (A) Cartoon schematic of the protein components used in gel filtration experiments below. Ndc80:Nuf2^{dwarf} was paired with a N-terminal truncated mutant of Spc24:Spc25. The black bars on Spc24 represent truncation sites. (B) Zoom in of the junction region showing residues that contact that nanobody (in purple sticks), and N-terminal truncation sites of Spc24. (C) Top panel: gel filtration chromatograms of Ndc80:Nuf2^{dwarf} combined with Spc24:Spc25. The fractions collected from 10.5 mL to 16 mL were analyzed by SDS-PAGE, bottom panel. The color of each chromatogram curve corresponds to the outline color of a box below. For example, the red curve corresponds to Ndc80:Nuf2^{dwarf} x Spc24:Spc25. There is no SDS-PAGE gel for the gold curve, Ndc80:Nuf2^{dwarf} x Spc24Δ8:Spc25.

Table S1, related to Experimental Procedures: X-ray diffraction data and refinement statistics.

	Ndc80C^{dwarf}	**Ndc80$^{e\text{-}dwarf}$**	**Ndc80$^{e\text{-}dwarf}$**
Name (number of data sets)	SeMet (1)	EMP (3)	$KPtCl_4$ (2)
Data collection [a]			
Space group	C 2 2 2_1	I 4_1 2 2	I 4_1 2 2
Cell dimensions			
a, b, c (Å)	169.4 186.6 122.0	226.3, 226.8, 237.3	229.4, 229.4, 233.3
α, β, γ (º)	90 90 90	90 90 90	90 90 90
Wavelength (Å)	0.9792	1.008	1.0396
Resolution (Å)	49.5 – 2.83	164. – 7.52	49.2 – 8.83
	(2.93 – 2.83)[b]	(7.72 – 7.52)	(9.88 –8.83)
R_{merge} (%)[c]	11.93 (144.1)	11.2 (217.7)	7.7 (122.7)
I/σI	10.8 (0.7)	14.0 (1.5)	15.2 (2.2)
Completeness %	100 (100)	100 (100)	99 (65)
Unique reflections	45973 (4292)	4140 (396)	4659 (359)
Redundancy	9.3 (8.2)	14.3 (15.5)	12.4 (14.7)
Refinement			
Resolution (Å)	49.5- 2.83	113. - 7.53	
No. of reflections	45968	4138	
R_{work} / R_{free}	.238/.265	.303/.312	
No. of atoms	11389	12667	
Protein	688	786	
Ligand/ion	1 (Mg^{2+})	6 Hg	
Water	39	-	
B factors			
Protein	85.	44.	
Ligand/ion	29. (Mg^{2+})	46.	
Water	49.	-	
R.m.s. deviations			
Bond lengths (Å)	0.003	0.007	
Bond angles (°)	0.58	0.97	

[a] Bijvoet pairs are treated separately for derivatives.

[b] Values in parentheses are for highest-resolution shell.

[C] Rmerge = ΣI(h,i) - <I(h)>I / Σ I(h,i), where <I(h)> is the mean intensity of the reflections.

SUPPLEMENTAL MOVIE 1 (related to Figure 4).

Hinge motion in Ndc80:Nuf2 "head".

SUPPLEMENTAL EXPERIMENTAL PROCEDURES

Molecular Cloning and Protein Purification

Ndc80c tetramers - The coding region of the shortened Ndc80 proteins – Ndc80, Nuf2, Spc24, and Spc25 -- were PCR amplified from codon optimized genes (GenScript), and cloned into a modified pET plasmid for co-expression, encoding a TEV protease cleavable hexahistidine (His_6) tag at the N-terminus of Ndc80 following a previously established cloning strategy (Schmitzberger and Harrison, 2012). All constructs encoding shortened Ndc80c proteins were made after this manner, except for is the construct encoding the proteins that make up $Ndc80c^{dwaf}$. In this construct, the Nuf2D4 gene is encoded with the following N-terminal tag: HHHHHHENLYFQSNASIFKDLEALSFQSNA (underlined residues are cleaved after digestion with TEV).

All proteins were made in *E. coli* strain Rosetta2 (DE3) pLys (Novagen) grown in 2x(YT) media at 37 °C to an optical density of 0.6 (absorption l = 600 nm) and then immediately induced by addition of isopropyl β-D-1-thiogalactopyranoside (IPTG) to a final concentration of 750 mM. After induction cells were grown at 18 °C for 18 hours before harvesting. Shortened versions of H_6-tagged Ndc80 were affinity purified from cell lysate with Co^{2+} resin (Talon Cobalt Resin, Clontech) using 1 mL of resin per 5 mg of His-tagged protein, followed by anion exchange chromatography using a HiTrap Q HP (GE Bioscience) column. SDS-PAGE analysis was used to confirm that the corresponding Nuf2, Spc24, and Spc25 proteins co-eluted with Ndc80. TEV protease with a C-terminal H_6 tag was added to the eluted sample to cleave the N-terminal H_6 tag of Ndc80 and passed again through Co^{2+} resin to clear the sample of digested product and protease. After digestion, the sample was concentrated and gel-filtered on a Superdex–S200 HiLoad 16/60 column (GE Healthcare) equilibrated with gel filtration (GF) in buffer consisting of 30 mM Hepes (4-(2-hydroxyethyl)-1-piperazineethanesulfonic acid), pH 7.6, 150 mM NaCl, and 5mM dithiothreitol. All shortened versions of Ndc80c (listed in the **Figure S1**) were gel filtered in this buffer except for $Ndc80c^{e\text{-}dwarf}$, for which the sodium chloride concentration was raised to 300 mM. All proteins were concentrated to approximately 15 mg/ml and immediately used for crystallization or binding experiments. Selenomethionyl $Ndc80c^{dwarf}$ was expressed in the same cells but grown in M9 minimal media (Sigma-Aldrich) to an O.D. of 0.6, at which point a mixture of six amino acids -- Leu, Ile, Phe, Ser, Thr and Val -- was added to the culture, and after equilibration, L(+)-selenomethionine (Acros Organics)(Van Duyne et al., 1993). Expression and purification continued as described above.

Nanobody **-** Nanobodies against a shortened Ndc80 complex were isolated from an immunized alpaca by a previously established method (Li et al., 2016). A total of eight nanbodies were isolated and screened for association with $Ndc80c^{e\text{-}dwarf}$. Each nanobody was cloned into a modified pET15b vector with conferring kanamycin resistance, expressed, and purified using the method described for the purification of shortened Ndc80c particles.

The $Ndc80^{e\text{-}dwarf}$:nanobody complex was assembled by combining purified $Ndc80c^{e\text{-}dwarf}$ and nanobody in a 1:2 molar ratio. Excess nanobody was separated from $Ndc80c^{e\text{-}dwarf}$ by gel filtration. SDS PAGE analysis confirmed that the major peak on the chromatogram contained all five peptides (nanobody, Ndc80, Nuf2, Spc24, and Spc25) in equimolar amounts.

Protein Crystallization and Data Collection

$Ndc80c^{dwarf/e\text{-}dwarf}$ Crystallization - Crystals grew in 48-well plates at 18°C by hanging-drop vapor diffusion method equilibrated against 200 mL of well solution, and cryopreserved in mother liquor supplemented with 25% glycerol. Selenomethionyl $Ndc80c^{dwarf}$ protein concentrated to 15 mg/ml crystallized in 1.2 – 1.7 M magnesium sulfate, 0.1 M MES (2-(*N*-morpholino)ethanesulfonic acid), pH 6.0 – 6.7. $Ndc80c^{e\text{-}dwarf}$: nanobody complex (in a 1:1 molar ratio) concentrated to 11 mg/ml crystallized in 12 – 16% polyethylene glycol 4,000, 0.1 M CHES (*N*-Cyclohexyl-2-aminoethanesulfonic acid), pH 9.0 – 9.4. The $Ndc80^{dwarf}$ crystals were in space group $C222_1$ (a=169.4 b=186.6, c=122.0); those of the $Ndc80^{e\text{-}dwarf}$:nanobody complex were in space group $I4_122$ (a=226.282, 226.82, 237.26).

Heavy Atom Soaks **–** Crystals of $Ndc80c^{e\text{-}dwarf}$ were transferred to sitting-well plates and soaked in the crystallization drop containing 0.1 mM ethyl mercuric phosphate (EMS) or 0.1 mM tetrachloroplatinate(II) for eight hours. After soaking, crystals were briefly back soaked in stabilization buffer before cryoprotecting.

Data Collection – All X-ray diffraction experiments were carried out the Advanced Photon Source, Argonne National Laboratory, on NE-CAT beamline 24-ID-C in the continuous vector scanning mode. Reflections from $Ndc80^{dwarf}$ crystals were measured at a wavelength of 0.9792 Å, EMS soaked $Ndc80^{e\text{-}dwarf}$ crystals at 1.008 Å, and tetrachloroplatinate(II) soaked $Ndc80^{e\text{-}dwarf}$ crystals at 1.0396 Å.

X-ray Structure Determination

Reflections were processed in XDS (Kabsch, 2010). All data sets were truncated at the resolution for which the $CC_{1/2}$ for the data reached 0.3 (Wang and Wing, 2014). Data were scaled and merged in the program Aimless from the CCP4 suite (Winn et al., 2011). The $Ndc80^{dwarf}$ structure was determined by the single anomalous dispersion method, locating 17 selenomethionine sites from their anomalous differences using the Shelx pipline and reflections to a minimum Bragg spacing of 3.4 Å (Sheldrick, 2010). Phase extension to 2.8 Å was carried out in DM using a stepwise resolution strategy (Winn et al., 2011). The initial map was used to produce a partial model with the Phenix AutoBuild software (Adams et al., 2010). Iterative rounds of model building in Coot (Emsley et al., 2010) and solvent flattening in RESOLVE (Terwilliger, 2000), using coordinates from the model to calculate a protein mask, yielded improved phases for further model building. The model was refined against the diffraction data using REFMAC5 (Murshudov et al., 1997) and Phenix (Adams et al., 2010). In the late stages of refinement, hydrogen bonds and TLS parameters were included as restraints (Painter and Merritt, 2006). Phases for the $Ndc80^{e\text{-}dwarf}$ structure were calculated by locating 6 Hg sites on the basis of their associated anomalous difference using the program HKL2MAP (Sheldrick, 2010) followed by density modification in Phaser (McCoy, 2007). Different parts of the $Ndc80^{dwarf}$ structure were placed into the initial map by MOLREP (Winn et al., 2011). Where needed, parts of the model were adjusted or built, guided by the Hg constellations, in Coot and O (Emsley et al., 2010; Jones et al., 1991); iterative rounds of model adjustment and density modification in Phaser followed (McCoy, 2007). A homology model of the nanobody, lacking CDR loop residues 28-32, 61-64, 103-115, and 129 -139, was placed into the electron density by MOLREP (CCP4 program suite: Winn et al., 2011), and the final model was refined in Phenix against the diffraction data. The platinum sites were located in Phaser (McCoy, 2007) using a combination of platinum anomalous signal and a partial model of $Ndc80c^{e\text{-}dwarf}$. The platinum sites confirmed our placement of 5 methionine residues in the $Ndc80^{e\text{-}dwaf}$ structure. The stereochemistry of the final structures was analyzed with Coot and MolProbity (Chen et al., 2010; Emsley et al., 2010). Ramachandran-plot statistics for $Ndc80c^{dwarf}$ were 97% favored, and 3% allowed.

Binding Experiments using Size Exclusion Chromatography

All analytical size exclusion chromatography experiments were performed at 4 °C using a Superdex-S200 Increase 10/300 GL column (GE Healthcare). Samples were mixed at 1:1 molar ratio, and equilibrated at room temperature for 30 minutes before injecting into the column in a final volume of 200 uL. The SEC buffer in all binding experiments consisted of 300 mM NaCl, 30 mM Hepes, pH 7.6, and 1 mM tris(2-carboxyethyl)phosphine (TCEP). The eluted volume was collected in fractions, which were analyzed by SDS-PAGE stained with Coomassie blue.

Structure Analysis, Sequence Alignments, and Figure Preparation

Solvent accessible area was calculated using the program AREAIMOL, and residues with a less than 30% solvent accessible area in a GXG tripeptide environment were classified as buried (Winn et al., 2011). Structures were aligned using Superpose in CCP4 or Lsq in O (Jones et al., 1991; Winn et al., 2011). The central helical axis of the coiled-coil region was determined using the program TWISTER (Strelkov and Burkhard, 2002). All protein sequences were aligned with T-Coffee (Notredame et al., 2000) and figures were prepared with PyMol (http://www.pymol.org/).

SUPPLEMENTAL REFERENCES

Adams, P.D., Afonine, P.V., Bunkoczi, G., Chen, V.B., Davis, I.W., Echols, N., Headd, J.J., Hung, L.W., Kapral, G.J., Grosse-Kunstleve, R.W., *et al.* (2010). PHENIX: a comprehensive Python-based system for macromolecular structure solution. Acta Crystallogr D Biol Crystallogr *66*, 213-221.

Chen, V.B., Arendall, W.B., 3rd, Headd, J.J., Keedy, D.A., Immormino, R.M., Kapral, G.J., Murray, L.W., Richardson, J.S., and Richardson, D.C. (2010). MolProbity: all-atom structure validation for macromolecular crystallography. Acta Crystallogr D Biol Crystallogr *66*, 12-21.

Emsley, P., Lohkamp, B., Scott, W.G., and Cowtan, K. (2010). Features and development of Coot. Acta Crystallogr D Biol Crystallogr *66*, 486-501.

Jones, T.A., Zou, J.Y., Cowan, S.W., and Kjeldgaard, M. (1991). Improved methods for building protein models in electron density maps and the location of errors in these models. Acta Crystallogr A *47 (Pt 2)*, 110-119.

Kabsch, W. (2010). XDS. Acta Crystallogr D Biol Crystallogr *66*, 125-132.

Li, L., Park, E., Ling, J., Ingram, J., Ploegh, H., and Rapoport, T.A. (2016). Crystal structure of a substrate-engaged SecY protein-translocation channel. Nature *531*, 395-399.

McCoy, A.J. (2007). Solving structures of protein complexes by molecular replacement with Phaser. Acta Crystallogr D Biol Crystallogr *63*, 32-41.

Murshudov, G.N., Vagin, A.A., and Dodson, E.J. (1997). Refinement of macromolecular structures by the maximum-likelihood method. Acta Crystallogr D Biol Crystallogr *53*, 240-255.

Notredame, C., Higgins, D.G., and Heringa, J. (2000). T-Coffee: A novel method for fast and accurate multiple sequence alignment. J Mol Biol *302*, 205-217.

Painter, J., and Merritt, E.A. (2006). Optimal description of a protein structure in terms of multiple groups undergoing TLS motion. Acta Crystallogr D Biol Crystallogr *62*, 439-450.

Schmitzberger, F., and Harrison, S.C. (2012). RWD domain: a recurring module in kinetochore architecture shown by a Ctf19-Mcm21 complex structure. EMBO Rep *13*, 216-222.

Sheldrick, G.M. (2010). Experimental phasing with SHELXC/D/E: combining chain tracing with density modification. Acta Crystallogr D Biol Crystallogr *66*, 479-485.

Strelkov, S.V., and Burkhard, P. (2002). Analysis of alpha-helical coiled coils with the program TWISTER reveals a structural mechanism for stutter compensation. J Struct Biol *137*, 54-64.

Terwilliger, T.C. (2000). Maximum-likelihood density modification. Acta Crystallogr D Biol Crystallogr *56*, 965-972.

Van Duyne, G.D., Standaert, R.F., Karplus, P.A., Schreiber, S.L., and Clardy, J. (1993). Atomic structures of the human immunophilin FKBP-12 complexes with FK506 and rapamycin. J Mol Biol *229*, 105-124.

Wang, J., and Wing, R.A. (2014). Diamonds in the rough: a strong case for the inclusion of weak-intensity X-ray diffraction data. Acta Crystallogr D Biol Crystallogr *70*, 1491-1497.

Winn, M.D., Ballard, C.C., Cowtan, K.D., Dodson, E.J., Emsley, P., Evans, P.R., Keegan, R.M., Krissinel, E.B., Leslie, A.G., McCoy, A., *et al.* (2011). Overview of the CCP4 suite and current developments. Acta Crystallogr D Biol Crystallogr *67*, 235-242.